



This is a repository copy of *Predictive hazard level assessment of Li-ion cell thermal runaway failure*.

White Rose Research Online URL for this paper:

<https://eprints.whiterose.ac.uk/206167/>

Version: Accepted Version

---

**Proceedings Paper:**

Bugryniec, P.J. [orcid.org/0000-0003-3494-5646](https://orcid.org/0000-0003-3494-5646) and Brown, S.F. (2024) Predictive hazard level assessment of Li-ion cell thermal runaway failure. In: Energy Storage Conference 2023 (ESC 2023). Energy Storage Conference 2023 (ESC 2023), 15-16 Nov 2023, Glasgow, United Kingdom. The Institution of Engineering & Technology . ISBN 9781839539985

<https://doi.org/10.1049/icp.2023.3096>

---

This paper is a postprint of a paper submitted to and accepted for publication in Energy Storage Conference 2023 (ESC 2023) and is subject to Institution of Engineering and Technology Copyright. The copy of record is available at the IET Digital Library.

**Reuse**

Items deposited in White Rose Research Online are protected by copyright, with all rights reserved unless indicated otherwise. They may be downloaded and/or printed for private study, or other acts as permitted by national copyright laws. The publisher or other rights holders may allow further reproduction and re-use of the full text version. This is indicated by the licence information on the White Rose Research Online record for the item.

**Takedown**

If you consider content in White Rose Research Online to be in breach of UK law, please notify us by emailing [eprints@whiterose.ac.uk](mailto:eprints@whiterose.ac.uk) including the URL of the record and the reason for the withdrawal request.



[eprints@whiterose.ac.uk](mailto:eprints@whiterose.ac.uk)  
<https://eprints.whiterose.ac.uk/>

# Predictive Hazard Level Assessment of Li-ion Cell Thermal Runaway Failure

Peter J Bugryniec<sup>1</sup>, Solomon F Brown<sup>1\*</sup>

<sup>1</sup>Department of Chemical and Biological Engineering, The University of Sheffield, Sheffield, UK

\*E-mail: s.f.brown@sheffield.ac.uk

**Keywords:** Statistical Analysis, Monte Carlo, Abuse Simulation, Lithium Ion Battery, Risk Assessment

## Abstract

Li-ion batteries (LIBs) are a widely adopted energy storage device that are increasingly used in transportation and stationary applications. However, LIBs come with the risk of thermal runaway (TR) which is known to be unpredictable. Previous computational work has assessed the sensitivity of TR to model inputs, while some experimental work has quantified the distribution of TR behaviour. However, no work is known to have used computational simulations of cell abuse to predict the probability of cell failure under typical abuse test standards. This work applies an abuse model to achieve this, as well as using key TR output variables to calculate the magnitude of cell failure according to the redefined EUCAR hazard level assessment. Abuse simulations of Underwriter Laboratory's oven test are simulated thousands of times considering parameter distributions with two different coefficient of variance sets. This work shows that it is possible to predict the change in the probability of failure against the change in oven temperature and the probability of different hazard levels. However, there is a need to better understand and refine the variance in cell parameters, specifically those related to the kinetic behaviour, to allow for analysis that is more suitable for risk assessment purposes.

## 1 Introduction

Li-ion batteries (LIBs) are an essential technology for enabling the UK, and other countries alike, to achieve Net Zero targets [1]. As an electrochemical energy storage device, LIBs achieve emissions reduction by enabling electrified powertrains which have improved efficiencies over internal combustion counterparts and through utilising relatively low carbon grid energy. Further, LIBs support the installation and utilisation of renewable energy through grid support services.

However, LIBs suffer from the potential to undergo thermal runaway (TR), which can lead to intense heat and fire that can destroy the entire battery system as well as be a hazard to people and assets within the vicinity [2]. Further, the accumulation of flammable gases can lead to explosions, while carbon monoxide and fluorinated gas species present a serious toxicity hazard. As such, ongoing research is required to better understand the TR processes and develop safer LIBs.

The TR and TR propagation of single cells and small modules has been greatly studied, with temperature profiles and gas emissions from failure quantified and mitigation measures assessed. However, it is widely known within the LIB and battery safety community that the TR behaviour on a larger scale, such as packs, is unpredictable. It is difficult to know when failure will occur and how severely it will progress.

The variation of TR severity (i.e. maximum temperature) and time to TR have been shown by several literature sources [3–5] for cells of different chemistries under accelerated rate calorimetry, oven exposure and constant power heating. A limited number of sources have calculated probability densities for maximum temperature, temperature rate and mass loss [6], and

also for the energy released by the ejecta, electrode and body components [7].

Computational modelling has been used for statistical studies on abuse and non-abusive scenarios. For abuse modelling, the decomposition heat generation sub-model (based on kinetic reactions) is important. Shah *et al.* [8] studied the effect of the solid electrolyte interphase kinetic parameters on TR behaviour but is limited by the lack of variation in other kinetics parameters. Kriston *et al.* [9] carried out an in-depth investigation on the uncertainty of LIB TR model parameters, including all kinetic parameters. They determined the most influential parameters on TR severity are internal short resistance ratio, cooling power, electrolyte combustion and the heat release from anode decomposition. Kriston *et al.* [9] considered the probability distribution of heat released from a cell determined experimentally to study heat transfer in a pack. But they only considered one reactive cell, and initiation is not based on kinetic equations. Xia *et al.* [10] studied the change in thermal safety boundary, considering the variation in cell properties. They showed that with increased degradation and internal resistance, the ability to maintain thermal safety is reduced. Huang *et al.* [11] determined TR initiation and propagation are highly dependent on heat capacity and thermal contact. Yeadly *et al.* [12] use a Gaussian Process surrogate model to analyse the sensitivity of cell thermal runaway given thermo-physical properties. It is found that emissivity, followed by convection and conductivity properties, plays the most significant role in key TR outputs (e.g. onset time and maximum temperature).

The existing literature has presented a useful discussion of the sensitivity analysis of TR models, determining the most influential parameters on TR severity. However, no known

work has used actual or assumed variations in the properties of manufactured cells to make statistical predictions of when a cell will fail.

Therefore, this work aims to determine the probability of cell failure given the variations in cell properties. The objectives are:

1. Use an existing Li-ion cell TR abuse model to simulate a recognised standard (overheat) safety test and categorise the TR event against EUCAR hazard levels;
2. Predict the frequency at which different hazard levels occur, assuming parameters have a normal distribution with known and speculated coefficients of variance, for the standard safety test; and
3. Determine the probability of cell failure at different oven exposer temperatures.

## 2 Methodology

This work considers a fully charged lithium cobalt oxide 18650 cylindrical cell as a case study for the hazard level assessment accounting for uncertainty. To simulate the abuse behaviour we apply the classical 4 reaction thermal runaway model as described by Kim *et al.* [13]. The governing equations of this model are presented in Section 2.1. Section 2.2 presents the values of parameters that are considered uncertain, along with their coefficient of variance. Section 2.3 describe the thermal abuse scenario simulated and the criteria for the hazard level assessment.

### 2.1 Thermal Runaway Modelling

The temperature of the cell for a lumped heat capacity model is governed by:

$$\rho C_p V_{cell} \frac{dT}{dt} = Q_{conv} + Q_{rad} + Q_{decomp} \quad (1)$$

where  $\rho$  ( $\text{kg m}^{-3}$ ) is the density of the cell,  $C_p$  ( $\text{J kg}^{-1} \text{K}^{-1}$ ) is the heat capacity of the cell,  $V_{cell}$  ( $\text{m}^3$ ) is the volume of the cell,  $T$  (K) is the temperature of the cell,  $t$  (s) is time,  $Q_{conv}$ ,  $Q_{rad}$  and  $Q_{decomp}$  ( $\text{J s}^{-1}$ ) are the heat generation/ dissipation from convection, radiation and TR decomposition respectively.

The heat transfer to/from the environment by radiation and convection are governed by:

$$Q_{conv} = A_{cell} h_{conv} (T_{oven} - T) \quad (2)$$

$$Q_{rad} = A_{cell} \varepsilon_{rad} \sigma_{rad} (T_{oven}^4 - T^4) \quad (3)$$

where  $A_{cell}$  ( $\text{m}^2$ ) is the surface area of the cylindrical cell,  $h_{conv}$  ( $\text{J s}^{-1} \text{m}^{-2} \text{K}^{-1}$ ) is the natural convection coefficient,  $T_{amb}$  (K) is the ambient or oven temperature,  $\varepsilon_{rad}$  (unit-less) is the radiation heat transfer coefficient,  $\sigma_{rad}$  ( $\text{J s}^{-1} \text{m}^{-2} \text{K}^{-4}$ ) is the Stefan–Boltzmann constant.

The decomposition heat generation is the sum of the heat from the solid electrolyte interphase (sei), negative-electrode/

electrolyte (ne), positive-electrode/ electrolyte (pe) and electrolyte (ele) reactions:

$$Q_{decomp} = (S_{sei} + S_{ne} + S_{pe} + S_{ele}) V_{jelly} \quad (4)$$

where  $V_{jelly}$  ( $\text{m}^3$ ) is the volume of the jelly roll and  $S_i$  ( $\text{J s}^{-1} \text{m}^{-3}$ ) is the specific heat generation of each reaction  $i$  given by:

$$S_{sei} = R_{sei} W_c H_{sei} \quad (5)$$

$$S_{ne} = R_{ne} W_c H_{ne} \quad (6)$$

$$S_{pe} = R_{pe} W_p H_{pe} \quad (7)$$

$$S_{ele} = R_{ele} W_e H_{ele} \quad (8)$$

where  $R_i$  ( $\text{s}^{-1}$ ) is the reaction rate,  $W_i$  ( $\text{g m}^{-3}$ ) is the specific mass of reactant and  $H_i$  ( $\text{J g}^{-1}$ ) is the heat of reaction for each reaction  $i$ .

The reaction rates,  $R_i$ , are governed by Arrhenius equations:

$$R_{sei} = A_{sei} e^{(-E_{a,sei}/R_{gas}T)} C_{sei}^{m_{sei}} \quad (9)$$

$$R_{ne} = A_{ne} e^{(-E_{a,ne}/R_{gas}T)} C_{ne}^{m_{ne}} e^{(-t_{sei}/t_{sei0})} \quad (10)$$

$$R_{pe} = A_{pe} e^{(-E_{a,pe}/R_{gas}T)} C_{pe}^{m_{pe1}} (1 - C_{pe})^{m_{pe2}} \quad (11)$$

$$R_{ele} = A_{ele} e^{(-E_{a,ele}/R_{gas}T)} C_{ele}^{m_{ele}} \quad (12)$$

where  $A_i$  ( $\text{s}^{-1}$ ) is the frequency factor,  $E_{a,i}$  ( $\text{J mol}^{-1}$ ) is the activation energy,  $R_{gas}$  ( $\text{J s}^{-1} \text{m}^{-2} \text{K}^{-4}$ ) is the Stefan–Boltzmann constant,  $C_i$  (unit-less) is the concentration of the decomposition species,  $t_{sei}$  and  $t_{sei0}$  are the non-dimensional thickness and initial thickness of the SEI,  $m_i$  is a non-dimensional power term.

The change in species concentrations,  $C_i$  and  $t_{sei}$ , are determined by:

$$dC_{sei}/dt = -R_{sei} \quad (13)$$

$$dC_{ne}/dt = -R_{ne} \quad (14)$$

$$dt_{sei}/dt = R_{ne} \quad (15)$$

$$dC_{pe}/dt = R_{pe} \quad (16)$$

$$dC_{ele}/dt = -R_{ele} \quad (17)$$

Throughout all simulations, the initial values of the dependent variables and the power terms  $m_i$  are fixed. The initial species concentrations are  $C_{sei} = 0.15$ ,  $C_{ne} = 0.75$ ,  $t_{sei} = 0.033$ ,  $C_{pe} = 0.04$  and  $C_{ele} = 1$  [13]. All the terms  $m_i$  are equal to 1 [13]. The initial cell temperature is 35°C and the oven set temperature is 150°C according to the testing criteria in Section 2.3. The values and variation in the other parameters are discussed in Section 2.2 below.

### 2.2 Parameter Distributions

The parameter values for the model (see Table 1) are taken from Ref. [13], and are assumed to represent the mean values for a batch of cells assuming a normal distribution. The variation in

Table 1 Model parameter values and coefficient of variation for Case 1 (measured) and Case 2 (assumed).

Parameter	Mean	CoV (meas.)	CoV (assu.)
$h_{conv}$ [ $\text{J s}^{-1} \text{m}^{-2} \text{K}^{-1}$ ]	7.17	0.05	
$\varepsilon_{rad}$ [-]	0.8	0.01	
$r_{cell}$ [mm]	9	0.01	
$h_{cell}$ [mm]	65	0.01	
$V_{jelly}$ [ $\text{m}^3$ ]	$1.052 \times 10^{-5}$	0.01	
$\rho C_p$ (cell) [ $\text{kg m}^{-3}$ ]	$2.5 \times 10^6$	0.05	
$E_{a,sei}$ [ $\text{J mol}^{-1}$ ]	$1.3508 \times 10^5$		
$E_{a,ne}$ [ $\text{J mol}^{-1}$ ]	$1.3508 \times 10^5$	0.14	
$E_{a,pe}$ [ $\text{J mol}^{-1}$ ]	$1.396 \times 10^5$		
$E_{a,ele}$ [ $\text{J mol}^{-1}$ ]	$2.74 \times 10^5$		0.01
$A_{sei}$ [ $\text{s}^{-1}$ ]	$1.667 \times 10^{15}$		
$A_{ne}$ [ $\text{s}^{-1}$ ]	$2.5 \times 10^{13}$	0.28	
$A_{pe}$ [ $\text{s}^{-1}$ ]	$6.667 \times 10^{13}$		
$A_{ele}$ [ $\text{s}^{-1}$ ]	$5.14 \times 10^{25}$		
$H_{sei}$ [ $\text{J g}^{-1}$ ]	257		
$H_{ne}$ [ $\text{J g}^{-1}$ ]	1714	0.11	
$H_{pe}$ [ $\text{J g}^{-1}$ ]	314		
$H_{ele}$ [ $\text{J g}^{-1}$ ]	155		
$W_c$ [ $\text{g m}^{-3}$ ]	$6.104 \times 10^5$		
$W_p$ [ $\text{g m}^{-3}$ ]	$1.221 \times 10^6$	0.05	
$W_e$ [ $\text{g m}^{-3}$ ]	$4.069 \times 10^5$		

the distribution, stated as the coefficient of variation (CoV) is, in case 1, based on measured variations where possible, and in case 2 assumed to be 1%.

The value of  $\rho C_p$  is slightly altered here to adjust for the difference in model formulation respective to Ref. [13]. Here we assume a reaction volume of  $V_{jelly}$  within a cell volume  $V_{cell}$  rather than one single volume as in Ref. [13].

Regarding case 1, Kriston *et al.* [14] present values for the variation in kinetic parameters found from DSC/TGA experiments. Here, values for the CoV of the activation energy, frequency factor and heat of reaction are based on typical values found in Ref. [14]. The CoV of mass, density and heat capacity is from the analysis of cell data in Ref. [15]. Other parameters are assumed to have a CoV of 1%.

To determine the probability of TR, and assess the hazard level (see Section 2.3), 10000 parameters set are randomly generated and simulated.

### 2.3 Safety Test and Hazard Level Assessment

There are several national and international testing standards for Li-ion cells that assess safety through environmental (including thermal), mechanical, electrical and chemical abuse [16, 17]. For this work, the focus will be on thermal abuse tests, specifically thermal stability and overheating. Underwriters Laboratory defines the overheating abuse test as exposing a cell to a temperature of 150°C for 60 min [17]. It is under these conditions that we assess the probability of cell failure.

Table 2 Hazard levels for LIB abuse simulations.

Hazard Level	Description	Classification Criteria & Effect
0	No Effect	No exothermic reaction or thermal runaway. i.e. no increase in cell temperature above oven set temperature, no change in overall decomposition species, no heat generation. (This is determined to be at the limit of $\Delta T < 5^\circ\text{C}$ and $(dT/dt)_{max} < 1^\circ\text{C min}^{-1}$ )
1	n/a	n/a
2	n/a	n/a
3	n/a	n/a
4	Self-heating	Exothermic reactions, $\Delta T < 25^\circ\text{C}$ and $(dT/dt)_{max} < 10^\circ\text{C min}^{-1}$
5	Mild Thermal Runaway	Exothermic reactions, $\Delta T < 50^\circ\text{C}$ and $(dT/dt)_{max} < 100^\circ\text{C min}^{-1}$
6	Moderate Thermal Runaway	Exothermic reactions, $\Delta T < 100^\circ\text{C}$ and $(dT/dt)_{max} < 1000^\circ\text{C min}^{-1}$
7	Severe Thermal Runaway	Exothermic reactions, $\Delta T \geq 100^\circ\text{C}$ or $(dT/dt)_{max} \geq 1000^\circ\text{C min}^{-1}$

The TR event has to first be categorised to allow the probability of failure to be assessed. Evaluation of battery safety under each test scenario is typically categorised against the EUCAR hazard level assessment [18]. This lists 8 hazard levels (0 – 7) as no effect, passive protection activated, defect/damage, leakage (less than 50% mass loss), venting (greater than 50% mass loss), fire, rupture and explosion.

As the EUCAR assessment is based on physical deformation characteristics and mass loss, which are physics currently not captured in the model, we have to redefine the classification criteria of the hazard level assessment. To be compatible with physical experiments (i.e. measurement capabilities) the classification criteria are based on the maximum temperature change of the cell given the oven set temperature (i.e.  $\Delta T = T_{cell,max} - T_{oven}$ ) and the maximum temperature rate (during the exothermic event). The refined hazard levels are presented in Table 2. The limits on classification criteria (governed by  $\Delta T$  and  $dT/dt$ ) are determined from experience, relating physical damage to temperature and temperature rate profiles.

## 3 Results

The base case scenario, using the parameters from Ref. [13], is presented in Fig. 1 and compared to the results of Kim *et al.* [13]. From this figure, it can be seen that the original results are reproduced accurately. Further, one can see that under the abuse condition (exposure in a 150°C oven for 60 min) self-heating/

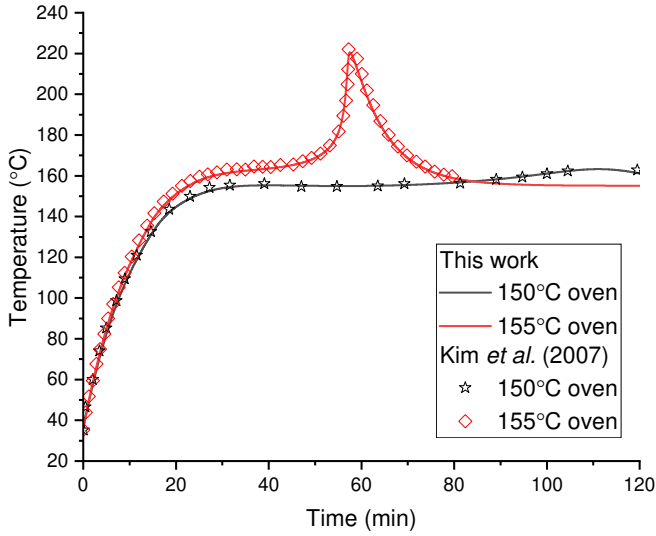
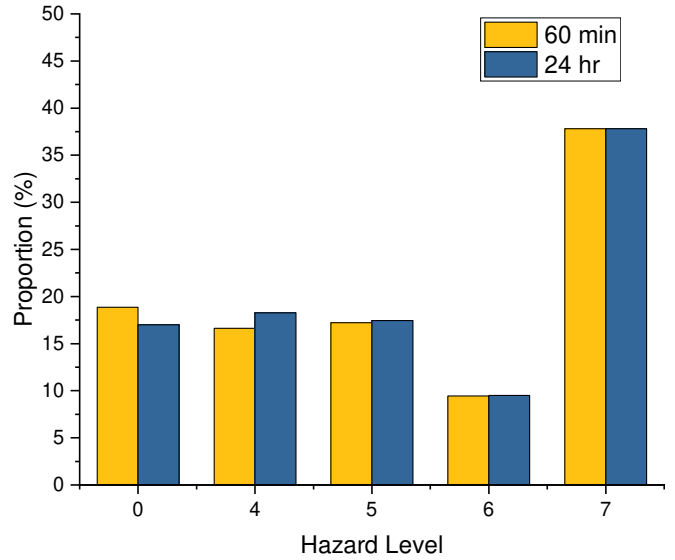


Fig. 1 Simulation of LCO 18650 cell TR under two oven set temperatures, where model parameters are set to those in Table 1 under the “Mean” column, and compared to original literature simulation of Kim *et al.* [13].

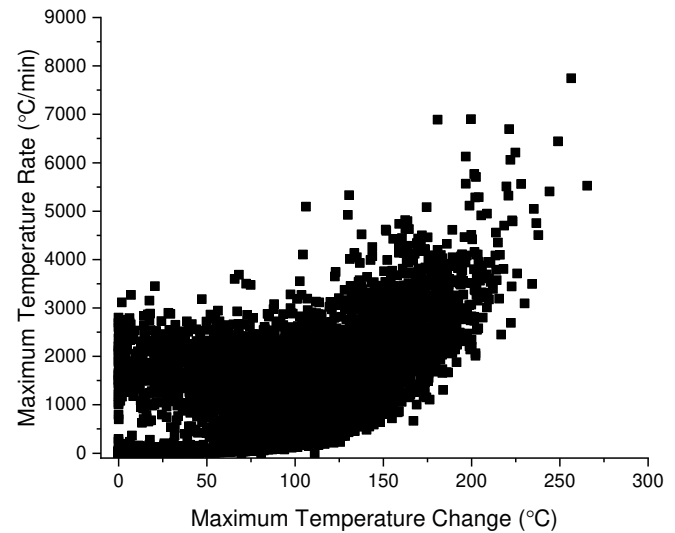
TR does not occur, hence the hazard level is 0. But at the time scale of 120 min it can be seen that self-heating does occur. Under this time frame the hazard level is 4, as the maximum temperature difference and temperature rate (of self-heating) are 5.3°C and 0.021°C min<sup>-1</sup> respectively. From this, it can be seen that the length of time a cell is monitored for under oven exposure is important. As such, in the following studies, the cells are assessed over a 60 min and 24 h period.

The results of the abuse simulations for Case 1 with “measured” CoV are presented in Fig. 2. The chart in Fig. 2(a) (for the 60 min exposure) shows a similar prediction of hazard levels 0, 4 and 5, at an occurrence of around 17% each. While hazard levels 6 and 7 account for approximately 10% and 37% of occurrences. The larger value of hazard level 7 can be reasoned from Fig. 2(b). Where it can be seen that there are occurrences of large temperature differences (>100°C) at lower maximum rates, and large maximum rates (>1000°C min<sup>-1</sup>) at very low temperature differences. The latter is the result of incidents where decomposition occurs at very low temperatures (i.e. ambient), leading to the rapid heating of the cell up to the oven-set temperature but with too little heat generation to raise it above the set temperature. Using Spearman’s Rank Correlation to analyse Fig. 2(b) it is found that no correlation can be calculated. The behaviour described above results in many occurrences that satisfy hazard level 7 by only one criterion. Further, comparing the 60 min and 24 h simulation periods in Fig. 2(a) we can see that there is a small shift (2%) of hazard level 0 predictions onto hazard levels 4 and 5.

The results of the abuse simulations for Case 2 with “assumed” CoV are presented in Fig. 3. The chart in Fig. 3(a) (for the 60 min exposure) shows that hazard level predictions are centred around level 4, with a significant number in hazard level 0. Unlike in Case 1, there is a clear correlation between the maximum rate and maximum temperature difference, see



(a)

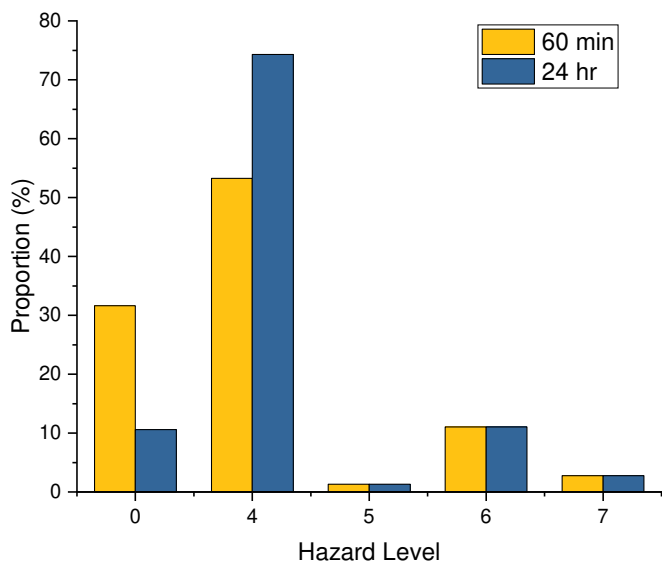


(b)

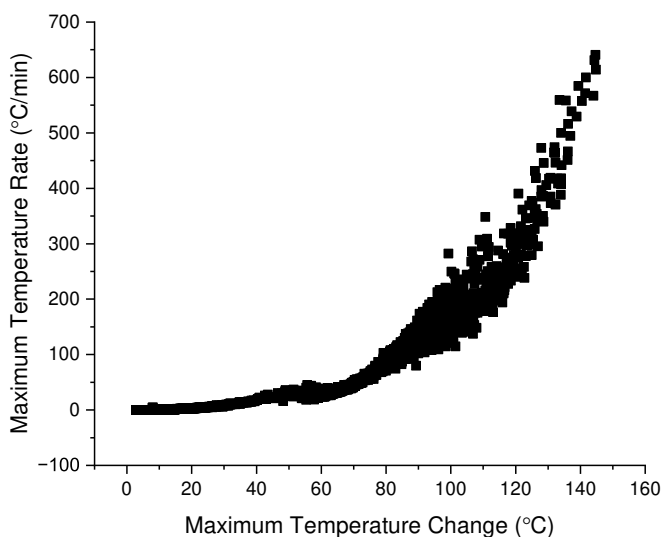
Fig. 2 Case 1 “measured” CoV: (a) calculated probability of each hazard level for two exposure times, (b) maximum cell temperature rate verse maximum cell temperature change over 60 min exposure.

Fig. 3(b). The Spearman’s Rank Correlation is calculated to be 0.87, with a p-value of 0. Further, it can be seen the absolute magnitude of the temperature difference and maximum rate is much lower in Case 2. With the maximum  $\Delta T$  being 150°C compared to 280°C and  $(dT/dt)_{max}$  being 750°C min<sup>-1</sup> compared to 9000°C min<sup>-1</sup>. Also, from Fig. 3(a) it can be seen that there is a significant shift (21%) from hazard level 0 to 4.

From the previous findings, it is clear that the CoV’s in Case 1 lead to behaviour in many instances that is not seen in published experimental literature. Resulting in the lack of expected correlation between maximum temperature and maximum temperature rate. As such, there is a need to refine the CoV’s of the cell parameters, especially the kinetic parameters as they



(a)



(b)

Fig. 3 Case 2 “assumed” CoV: (a) calculated probability of each hazard level for two exposure times, (b) maximum cell temperature rate verse maximum cell temperature change over 60 min exposure.

have the largest values. Conversely, Case 2 provides useful findings on the probability of different hazard levels, but importantly identifies that there is a need to consider the time period over which the assessment is done to ensure all failure events are captured. However, the CoV’s still need to be determined appropriately.

Further to the Underwriters Laboratory oven abuse test, the assessment was extended to predict the TR behaviour across a wide range of oven set temperatures, from ambient to 180°C. Note, as this study considered oven temperature as low as 20°C, the initial temperature of the cell was assumed to be 10°C so that it was below the lowest oven set temperature.

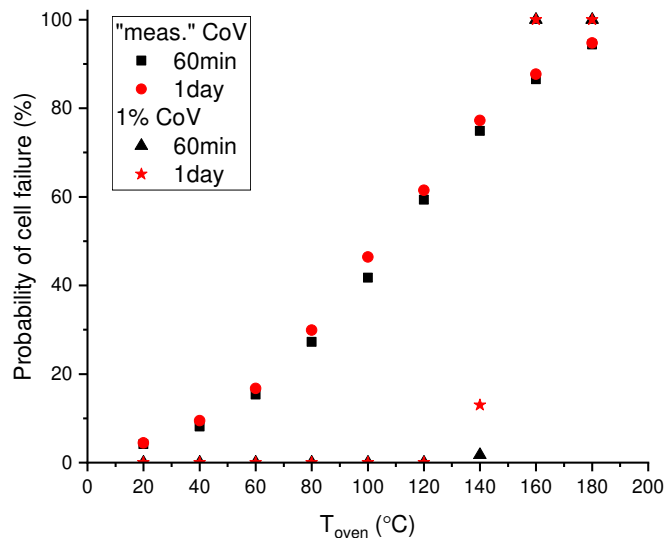


Fig. 4 Probability of cell failure (hazard level 4 or more) at various oven temperatures for the two CoV case studies. Both 60 min and 1 day exposure times presented.

The results of this study are presented in Fig. 4. As in the previous figures (Figs. 2(a) and 3(a)) both the 60 min and 24 h exposure times are presented. As before, analysis at longer exposure times is more important in Case 2, where there is a large difference at 140°C between the two exposure times. The figure also shows that, for Case 1, there is a 5% chance that a cell will fail at 20°C which steadily increases with exposure temperature. However, for Case 2 it can be seen that there is a shift from safe (0% failure) to unsafe (~100% failure) between 120°C and 160°C.

The notable chance of failure in Case 1 at the operational temperatures of LIBs (20°C to 60°C) identifies that the current CoV’s determined for the kinetic parameters are not calculated to enough certainty to provide meaningful predictions on safety or the probability of failure. However, Case 2 shows how this method can be utilised to predict the varying probability of cell failure under different conditions.

## 4 Conclusion

In this work, a classical Li-ion cell TR model is applied to simulate abuse and predict the resulting probability of cell failure and hazard level. Abuse simulations of Underwriter Laboratory’s oven test are simulated thousands of times considering parameter distributions with measured CoV’s from literature and assumed tighter values. From this, key output variables (maximum temperature change and maximum temperature rate) are used to calculate the magnitude of cell failure according to the redefined EUCAR hazard level assessment.

This work shows that it is possible to predict the change in probability of failure with oven temperature, and (for CoV’s of 1%) failure at 150°C is at hazard levels 0, 4 and 5–7 in 10%, 75% and 15% of occurrences. Furthermore, it shows that it is important to consider the oven exposure time so that all failure

events are captured. However, there is a need to better understand and refine the variance in cell parameters, specifically those related the kinetic behaviour, to allow for analysis that is more suitable for risk assessment purposes.

## 5 Acknowledgements

This work was supported by the Faraday Institution [grant number FIRG061].

## 6 References

- [1] Science and Technology Select Committee: ‘Battery strategy goes flat: Net-zero target at risk’, (Authority of the House of Lords, 2021)
- [2] McKinnon, M., DeCrane, S., Kerber, S.: ‘Four Firefighters Injured In Lithium-Ion Battery Energy Storage System Explosion - Arizona’, (Underwriters Laboratories, 2020)
- [3] Golubkov, A., Fuchs, D., Wagner, J., et al.: ‘Thermal-runaway experiments on consumer Li-ion batteries with metal-oxide and olivin-type cathodes’, *RSC Adv.*, 2014, 4, pp. 3633–3642
- [4] Bugryniec, P., Davidson, J., Cumming, D., et al.: ‘Pursuing safer batteries: Thermal abuse of LiFePO<sub>4</sub> cells’, *Journal of Power Sources*, 2019, 414, pp. 557–568
- [5] Zhang, L., Yang, S., Liu, L., et al.: ‘Cell-to-cell variability in Li-ion battery thermal runaway: Experimental testing, statistical analysis, and kinetic modeling’, *Journal of Energy Storage*, 2022, 56, pp. 106024
- [6] Buckwell, M., Kirchner-Burles, C., Owen, R., et al.: ‘Cell-to-cell variability in Li-ion battery thermal runaway: Experimental testing, statistical analysis, and kinetic modeling’, *Journal of Energy Storage*, 2023, 65, pp. 107069
- [7] Walker, W., Bayles, G., Johnson, K., et al.: ‘Evaluation of Large-Format Lithium-Ion Cell Thermal Runaway Response Triggered by Nail Penetration using Novel Fractional Thermal Runaway Calorimetry and Gas Collection Methodology’, *Journal of The Electrochemical Society*, 2022, 169, pp. 060535
- [8] Shah, K., Ankur, J.: ‘Prediction of thermal runaway and thermal management requirements in cylindrical Li-ion cells in realistic scenarios’, *International Journal of Energy Research*, 2019, 43, pp. 1827–1838
- [9] Kriston, A., Podias, A., Adanouj, I., et al.: ‘Analysis of the Effect of Thermal Runaway Initiation Conditions on the Severity of Thermal Runaway—Numerical Simulation and Machine Learning Studys’, *Journal of The Electrochemical Society*, 2020, 167, pp. 090555
- [10] Xia, Q., Ren, Y., Wang, Z., et al.: ‘Safety risk assessment method for thermal abuse of lithium-ion battery pack based on multiphysics simulation and improved bisection method’, *Energy*, 2023, 264, pp. 126228
- [11] Huang, C., Bisschop, R., Anderson, J.: ‘A Sensitivity Study of a Thermal Propagation Model in an Automotive Battery Module’, *Fire Technology*, 2023
- [12] Yearlly, A., Bugryniec, P., Milton, R., et al.: ‘A study of the thermal runaway of lithium-ion batteries: A Gaussian Process based global sensitivity analysis’, *Journal of Power Sources*, 2023, 456, pp. 228001
- [13] Kim, G., Pesaran, A., Spotnitz, R.: ‘A three-dimensional thermal abuse model for lithium-ion cells’, *Journal of Power Sources*, 2007, 170, pp. 476–489
- [14] Kriston, A., Adanouj, I., Ruiz, V., et al.: ‘Quantification and simulation of thermal decomposition reactions of Li-ion battery materials by simultaneous thermal analysis coupled with gas analysis’, *Journal of Power Sources*, 2019, 435, pp. 226774
- [15] Bugryniec, P.: ‘Experimental and Computational Analyses of Thermal Runaway in Lithium Iron Phosphate Cells and Battery Packs’, PhD Thesis, The University of Sheffield, 2021
- [16] Ruiz, V., Pfrang, A., Kriston, A., et al.: ‘A review of international abuse testing standards and regulations for lithium ion batteries in electric and hybrid electric vehicles’, *Renewable and Sustainable Energy Reviews*, 2018, 81, pp. 1427–1452
- [17] Chen, Y., Kang, Y., Zhao, Y., et al.: ‘A review of lithium-ion battery safety concerns: The issues, strategies, and testing standards’, *Journal of Energy Chemistry*, 2021, 59, pp. 83–99
- [18] Doughty, D., Crafts, C.: ‘FreedomCAR: electrical energy storage system abuse test manual for electric and hybrid electric vehicle applications’, (Sandia National Laboratories, 2006)